# Validation of the Steam Condensation Region Model (SCRM) for CFD Analysis of Steam Discharge in the IRWST

Sung Man Son<sup>a</sup>, Dae Kyung Choi<sup>a</sup>, Choengryul Choi<sup>a\*</sup>, Kwang-Chu Kim<sup>b</sup>.

<sup>a</sup> ELSOLTEC, Giheung-gu, Yongin, Gyeonggi-do, 16950, Korea

<sup>b</sup>KEPCO Engineering and Construction Co. Ltd.,269 Hyeoksin-ro, Gimcheon-si, Gyeongsangbuk-do, 39660, Korea

\*Corresponding author: crchoi@elsoltec.com

### \*Keywords: Steam Condensation Region Model (SCRM), IRWST, Sparger, CFD Simulation, Direct Contact Condensation

#### 1. Introduction

The In-Containment Refueling Water Storage Tank (IRWST) is a large pool installed inside the containment building of a nuclear power plant, serving as an essential safety system that supplies cooling water in emergency conditions (Fig. 1). Unlike the external Refueling Water Storage Tank (RWST), the IRWST is located inside the containment, providing protection against seismic or external hazards, and functions as the water source for both the Emergency Core Cooling System (ECCS) and the containment spray system. A sparger, installed within the IRWST, discharges steam directly into the pool, where it is rapidly condensed. This process effectively suppresses containment pressure while also mitigating noise and hydrodynamic loads. However, as the pool temperature increases, the condensation rate decreases and the steam pocket length extends, potentially imposing additional pressure loads on the tank wall and affecting structural integrity. Maintaining the pool temperature within an acceptable limit is therefore essential for safety.

Direct two-phase CFD simulations of steam—water interaction are, however, computationally demanding and complex. To overcome this limitation, this study applies the Steam Condensation Region Model (SCRM), which replaces the two-phase region with a simplified single-phase representation by defining a condensation zone where the mass, momentum, and energy of the discharged steam are treated. In this work, the SCRM is validated through CFD analyses of a single-nozzle experiment (Fig. 2) and a multi-nozzle sparger experiment (Fig. 3), and the results are compared with experimental data.

## 2. Analysis Methods

#### 2.1 SCRM

The Steam Condensation Region Model (SCRM) defines the condensation zone where steam and coolant are mixed, and incorporates the exchange of mass, momentum, and energy into the CFD governing equations as source terms (Fig. 4). This approach accounts for momentum loss and latent heat release due to steam condensation, while significantly reducing

computational cost compared to direct two-phase simulations, enabling efficient approximation of condensation behavior.

#### 2.2 Analysis Method

The analysis employed three-dimensional incompressible RANS equations and the energy equation, with turbulence effects considered using the Standard k-

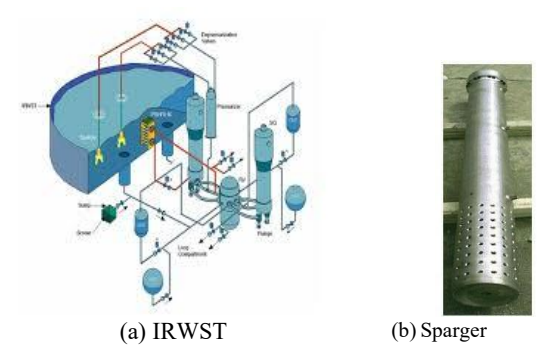


Fig. 1. IRWST schematic and sparger

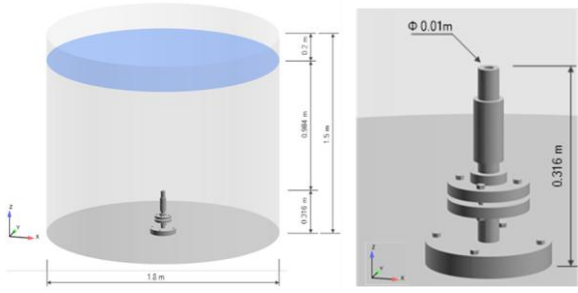


Fig. 2. Single-nozzle experiment

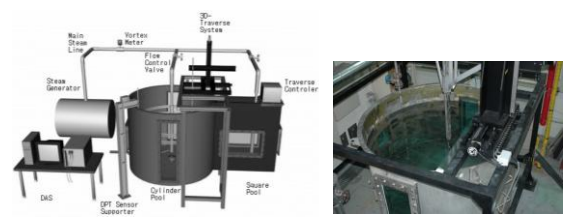


Fig. 3. Multi-nozzle experiment (sparger experiment)

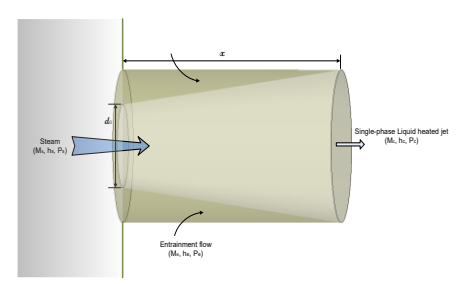


Fig. 4. Steam condensation region

Table I: Experimental conditions

	unit	Single-nozzle experiment	Multi-nozzle experiment				
Initial water level	[m]	1.30	3.65				
Initial temperature	[°C]	45	40				
Steam pressure	[MPa]	0.564	0.564				
Steam temperature	[°C]	156.4	156.4				
Steam discharge rate	[kg/m <sup>2</sup> s]	450	600				

 $\epsilon$  model and the  $k\text{-}\omega$  SST model to evaluate turbulence model sensitivity. Steam condensation was implemented through the Steam Condensation Region Model (SCRM), applied using a user-defined function (UDF) in ANSYS Fluent. The computational mesh consisted of approximately 2 million unstructured cells, and the experimental conditions are summarized in Table I. The SCRM was applied to the condensation region near the sparger discharge outlet.

The mesh employed in this study shows good agreement with the single- and multi-nozzle experimental results, ensuring the reliability of the SCRM analysis and making it suitable for simulating steam injection and condensation phenomena.

## 3. Results and Discussion

### 3.1 Single-nozzle experiment

Fig. 5 presents the flow vectors and temperature distribution resulting from single-nozzle steam injection. The upward-directed steam jet induces an entrainment flow of the surrounding fluid, and localized temperature rise along the jet path due to condensation can be observed.

Fig. 6 shows the axial velocity distribution along the radial distance at different measurement locations. Both the experimental results and CFD analysis capture the trend of high velocity at the jet center, followed by a rapid decrease in the radial direction. The two turbulence models (k- $\omega$  SST and Standard k- $\epsilon$ ) produced results that are qualitatively consistent with the experiments, with only minor differences between them.

Fig. 7 compares the axial velocity distribution along the jet axis. The CFD analysis reproduced the

experimental trend well, particularly the velocity decay behavior observed during jet attenuation. The influence of the turbulence model was found to be limited.

Table II provides a statistical comparison between experimental data and CFD results for different turbulence models. All cases showed a high correlation coefficient ( $r^2 > 0.96$ ) and low RMSE and MAE values, confirming that the CFD analysis reproduced the experimental results quantitatively with good accuracy.

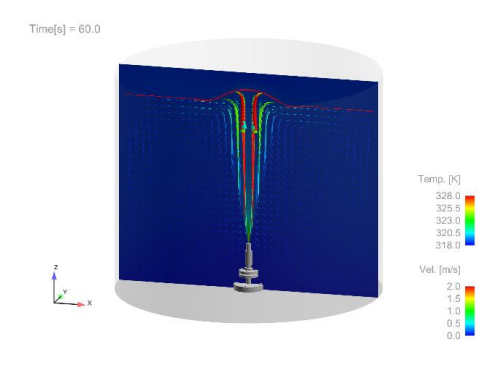


Fig. 5. Velocity vectors and temperature distribution

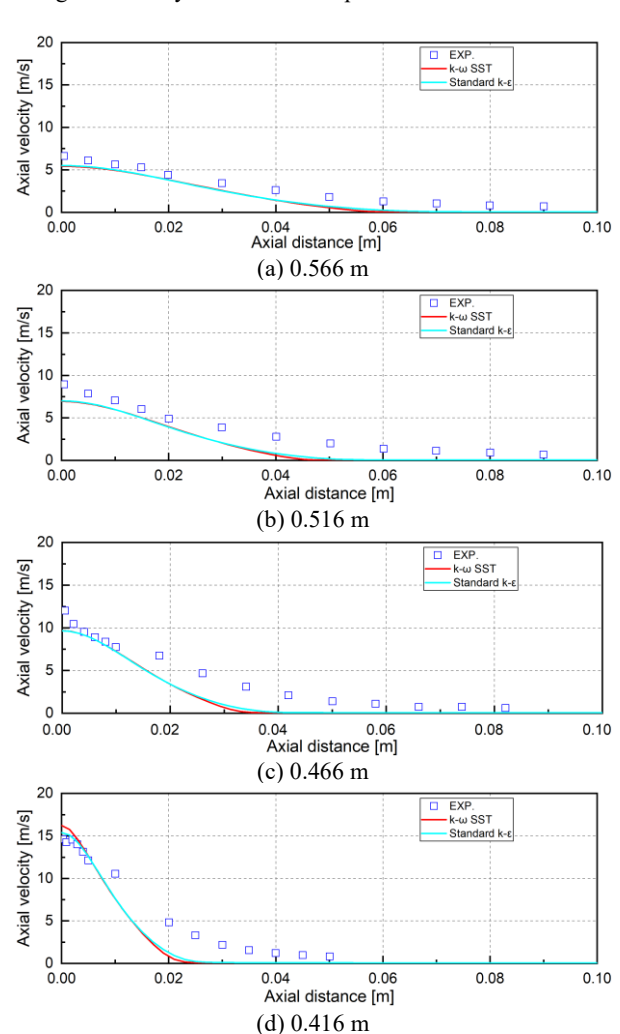


Fig. 6. Axial velocity along radial distance

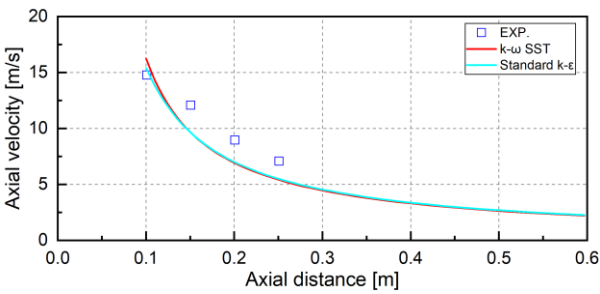


Fig. 7. Axial velocity along axis

The differences between the  $k\text{-}\omega$  SST and Standard  $k\text{-}\epsilon$  models were minimal, indicating that turbulence model selection had little impact on the overall results.

Table II: Statistical Comparison of Experimental Data

and CFD Results					
Vel.	Turbulenc e model	RD	RMSE	MAE	r
Radial	k-ω SST	0.533	1.481	1.292	0.983
	Standard k-ε	0.512	1.393	1.203	0.985
	k-ω SST	0.054	1.024	0.533	0.963
Axis	Standard k-ε	0.049	0.953	0.465	0.970

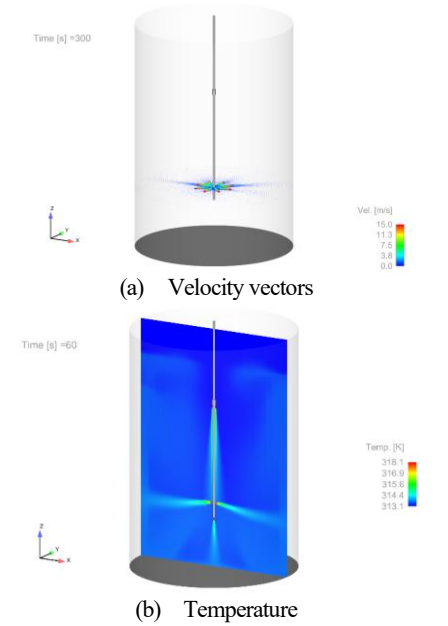


Fig. 8. Velocity vectors and temperature distribution

# 3.2 Multi-nozzle experiment (sparger experiment)

Fig. 8 illustrates the flow vectors and temperature distribution generated during steam discharge from the multinozzle sparger. The steam injection produces strong downward jets accompanied by entrainment of the surrounding fluid, while localized regions of elevated temperature appear along the jet path due to condensation.

Fig. 9 compares the temperature variations at each monitoring location in the GIRLS experiment with the CFD results. At all positions, the CFD analysis reproduced the

experimental trends qualitatively well, capturing the gradual increase in water temperature over time. Both the k- $\omega$  SST and Standard k- $\epsilon$  models showed good agreement with the

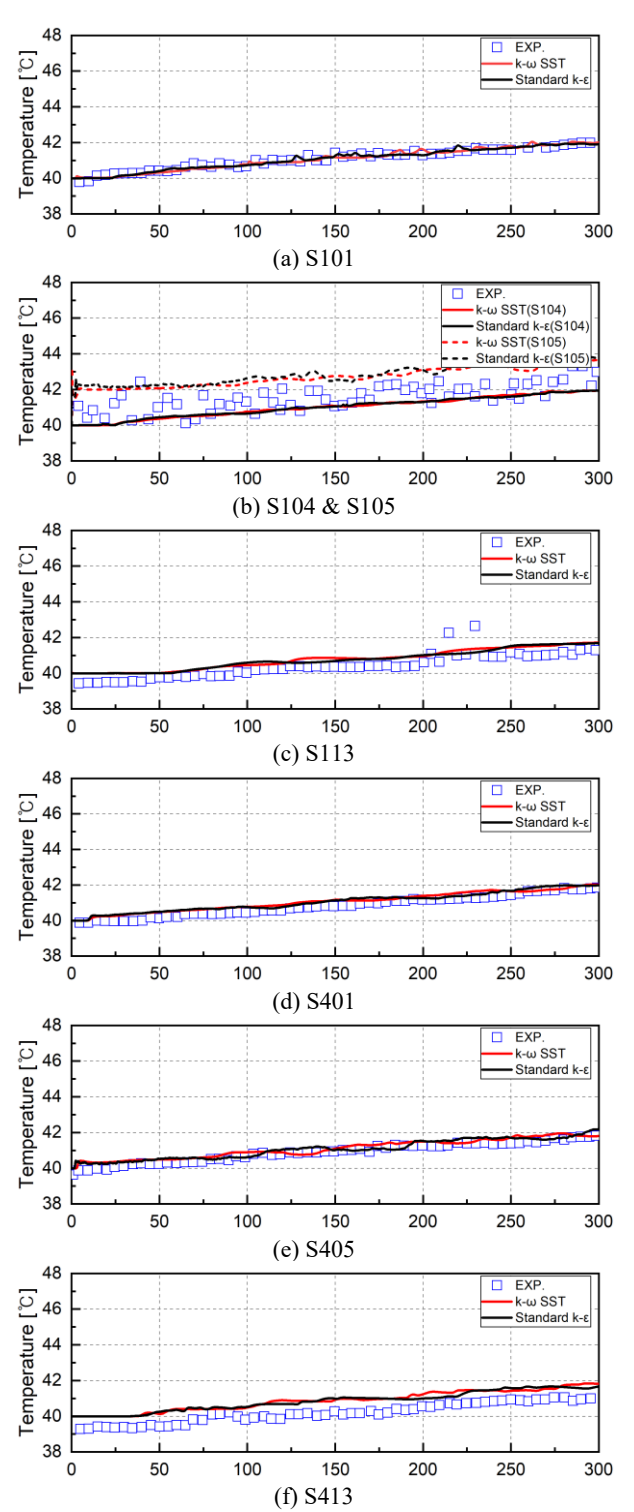


Fig. 9. Temperature results at each monitoring location

measurements, with only minor differences between them.

Tables III and IV summarize the comparisons of average, maximum, and minimum temperatures at the monitoring locations. The CFD results showed good quantitative

agreement with the experimental data, with negligible differences in average temperature. Maximum and minimum values were also well reproduced, and the differences between the two turbulence models were minimal. These results confirm that CFD analysis can be reliably applied to multi-nozzle sparger experiments.

Table III: Comparison of Experimental Data and CFD Results (a)

Temp.	Unit	S101		S104		S113	
		kωSS T	kε	kωSS T	kε	kωSS T	kε
AVG.	[°C]	40.74	40.75	40.71	40.72	40.5	40.48
MAX.	[°C]	42.05	41.94	41.94	41.94	41.72	41.69
MIN.	[℃]	40.0	40.0	40.0	40.0	40.0	40.0

Table IV: Comparison of Experimental Data and CFD Results (b)

Temp.	Unit	S401		S405		S413	
		kωSS T	kε	kωSS T	kε	kωSS T	kε
AVG.	[℃]	40.79	40.79	40.84	40.81	40.58	40.57
MAX.	[°C]	42.03	41.99	41.96	42.19	41.84	41.67
MIN.	[°C]	40.0	40.0	40.0	40.0	40.0	40.0

#### 4. Conclusions

In this study, the Steam Condensation Region Model (SCRM) was applied to analyze steam condensation behavior during steam discharge into the IRWST of a nuclear power plant, and its validity was verified using data from a single-nozzle experiment (BNC) and a multinozzle experiment (GIRLS).

The velocity and temperature distributions obtained from CFD showed good qualitative and quantitative agreement with the experimental results. Turbulence model sensitivity analysis indicated that the differences between the Standard k- $\epsilon$  model and the k- $\omega$  SST model were negligible, and that the dominant factor in predicting steam condensation behavior was the modeling of the condensation region rather than the choice of turbulence model.

Furthermore, compared with direct two-phase simulations, the SCRM approach significantly reduced computational cost while still reproducing the experimental results, confirming that single-phase CFD analysis with SCRM can be practically applied to design and safety assessments. Therefore, SCRM can serve as an effective method for analyzing steam condensation phenomena in pools such as the IRWST, and its accuracy is expected to be further improved through future analyses and comparisons with additional experimental data.

## REFFERENCES

- [1] H.Y. Kim, Y.Y. Bae, C.-H. Song, J.K. Park, S.M. Choi, "Experimental study on stable steam condensation in a quenching tank," *Int. J. Energy Res.*, 25(3), pp. 239-252 (2001).
- [2] X.-Z. Wu, J.-J. Yan, S.-F. Shao, Y. Cao, J.-P. Liu, "Experimental study on the condensation of supersonic

- steam jet submerged in quiescent subcooled water: steam plume shape and heat transfer," *Int. J. Multiphase Flow*, 33(12), pp. 1296-1307 (2007).
- [3] P.J. Kerney, G.M. Faeth, D.R. Olson, "Penetration characteristics of a submerged steam jet," *AIChE J.*, 18, pp. 548-553 (1972).
- [4] J.C. Weimer, G.M. Faeth, D.R. Olson, "Penetration of vapor jets submerged in subcooled liquids," *AIChE J.*, 19, pp. 552-558 (1973).
- [5] M.H. Chun, Y.S. Kim, J.W. Park, "An investigation of direct condensation of steam jet in subcooled water," *Int. Comm. Heat Mass Trans.*, 23(7), pp. 947-958 (1996).
- [6] R.E. Gamble, T.T. Nguyen, B.S. Shiralkar, P.F. Peterson, R. Greif, "Pressure suppression pool mixing in passive advanced BWR plants," *Nucl. Eng. Design*, 204, pp. 321-336 (2001).
- [7] F.M. White, *Viscous Fluid Flow*, 2nd ed., McGraw-Hill, New York (1991).
- [8] Y.T. Moon, "CFD simulation of steam jet induced thermal mixing in subcooled water pool," Ph.D. Thesis, Seoul National University (2009).
- [9] C.H. Song, Y.S. Kim, "Direct contact condensation of steam jet in a pool," *Advances in Heat Transfer*, Vol. 43, pp. 111-186 (2011).
- [10] C.K. Chan, C.K.B. Lee, "A regime map for direct contact condensation," *Int. J. Multiphase Flow*, 8(1), pp. 11-20 (1982).
- [11] S. Cho, C.-H. Song, C.K. Park, S.K. Yang, M.K. Chung, "Experimental study on dynamic pressure pulse in direct contact condensation of steam jets discharging into subcooled water," Proc. 1st Korea-Japan Symposium on Nuclear Thermal Hydraulics and Safety (NTHAS98), pp. 291-298 (1998).
- [12] A.P. De With, R.K. Calay, G. De With, "Three-dimensional condensation regime diagram for direct contact condensation of steam injected into water," *Int. J. Heat Mass Trans.*, 50, pp. 1762-1770 (2007).
- [13] X.-Z. Wu, J.-J. Yan, D.-D. Pan, G.-Y. Liu, W.-J. Li, "Condensation regime diagram for supersonic/sonic steam jet in subcooled water," *Nucl. Eng. Design*, 239, pp. 3142-3150 (2009).
- [14] S.S. Gulawani, J.B. Joshi, M.S. Shah, C.S. RamaPrasad, D.S. Shukla, "CFD analysis of flow pattern and heat transfer in direct contact steam condensation," *Chem. Eng.* Sci., 61(16), pp. 5204-5220 (2006).
- [15] H.S. Kang, C.H. Song, "CFD analysis for thermal mixing in a subcooled water tank under a high steam mass flux discharge condition," *Nucl. Eng. Design*, 238, pp. 492-501 (2008).
- [16] H.S. Kang, C.H. Song, "CFD analysis of turbulent jet behavior induced by a steam jet discharged through a vertical upward single hole in a subcooled water pool," *Nucl. Eng. Technol.*, 42(4), pp. 377-386 (2010).
- [17] C.H. Song, W.P. Baek, J.K. Park, "Thermal-hydraulic tests and analysis for the APR1400's development and licensing," *Nucl. Eng. Technol.*, 39(4), pp. 299-312 (2007).
- [18] C.K. Park, H.G. Jun, Y.J. Youn, C.H. Song, K.K. Lee, H.J. Ko, "Thermal mixing phenomena due to a steam injection into a cylindrical tank," *Proc. Korean Nuclear Society Autumn Meeting*, 2008.